Molecular View of Biomimetic Peptide in Action with Membrane

Jayakrishna Koneru, Dube Dheeraj Prakashchand, Namita Dube, Pushpita Ghosh, and Jagannath Mondal*

Tata Institute of Fundamental Research Hyderabad, 500046 India

E-mail: jmondal@tifrh.res.in,+914020203091

Abstract

Short-chain synthetically designed biomimetic peptides have recently emerged as the practical alternatives of naturally occurring antimicrobial peptides. A pertinent question in this regard is: how does the distinct molecular architecture of short synthetic peptides, compared to their relatively long and flexible natural antimicrobial counterpart, lead to potent membrane disruption ability ? Here, we address this question via computationally investigating the action of 10-residue-long β-peptide, a low-molecular weight synthetically designed antimicrobial foldamer, with a bacterial membrane-mimicking phospholipid bilayer. The investigation demonstrates that, beyond a threshold peptide-concentration, this short biomimetic peptide undergoes spontaneous self-aggregation and membrane-adsorption and subsequently forms stable transmembrane pore inside the membrane via a cooperative fashion, leading to membrane-disruption via water-leakage. Interestingly, the pore-inducing ability is found to be elusive in a non-globally amphiphilic sequence isomer, displaying its strong sequence-selective action on membrane. The analysis reveals that, despite having a short helical frame-work, these synthetic peptides, once inside the membrane, are able

to stretch themselves towards favourable potential contact with polar head groups and interfacial water layer, thereby facilitating membrane-spanning pore formation process. Taken together, this work brings out a distinct mechanism of membrane-activity of minimally designed synthetic biomimetic oligomers relative to the natural antimicrobial peptides.

Introduction

The development of bacterial resistance to conventional antibiotics is a major concern towards public health. Antimicrobial peptides, which provide a natural defence against a large range of pathogens, including bacteria and fungi, are emerging as a sustainable substitute of antibiotics. The peptide-based antimicrobial agents are less prone to bacterial resistance than the natural antimicrobial agents and have got well-deserved prominence.[1–4] However, serious issues with the naturally occurring antimicrobial peptides which have prevented their wide-spread appreciations are their susceptibility to degradation by cellular proteases and lack of specificity for microbial targets over host cells. In this regard, synthetic oligomers and synthetic peptides which adopt helical conformations, are coming up as a viable alternative to overcome these limitations of natural antimicrobial peptides.[5–8] The present work focuses on a promising class of potentially novel biomimetic anti-microbial synthetic peptides, referred as β-peptides and provides key molecular insights of the underlying mechanisms of their membrane-disruption capability.

β-peptides are synthetic oligomers of β-amino acids and are rationally designed to mimic and improve the biological activities of their natural counter parts, namely α-peptides. The backbone of a β-amino acid contains an additional carbon atom compared to that of α-amino acid, which provides an additional site for introducing side chain and makes the β-peptides resistant to degradation by natural proteases.[9] Synthetic oligomers and random copolymers of β amino acids[10,11] have shown potent antibacterial[12–14] and antifungal[15,16] activity. The synthetic peptide of our current interest is an amphiphilic 10-residue-length β-peptide sequence βY-(ACHC-ACHC-βK)$_3$ (hereby called 'AAK') where βY, βK and ACHC refer to β-tyrosine, β-lysine and trans-2-amino cyclohexyl carboxylic acid (see Figure 1). The cyclic constraint of ACHC residues confers a stable 14-helical conformation to this significantly short β-peptide sequence.

The ability to form stable 14-helical amphiphilic conformation by only ten β-amino acid residues provides the peptide a greater synthetic advantage over relatively long-chain natu-

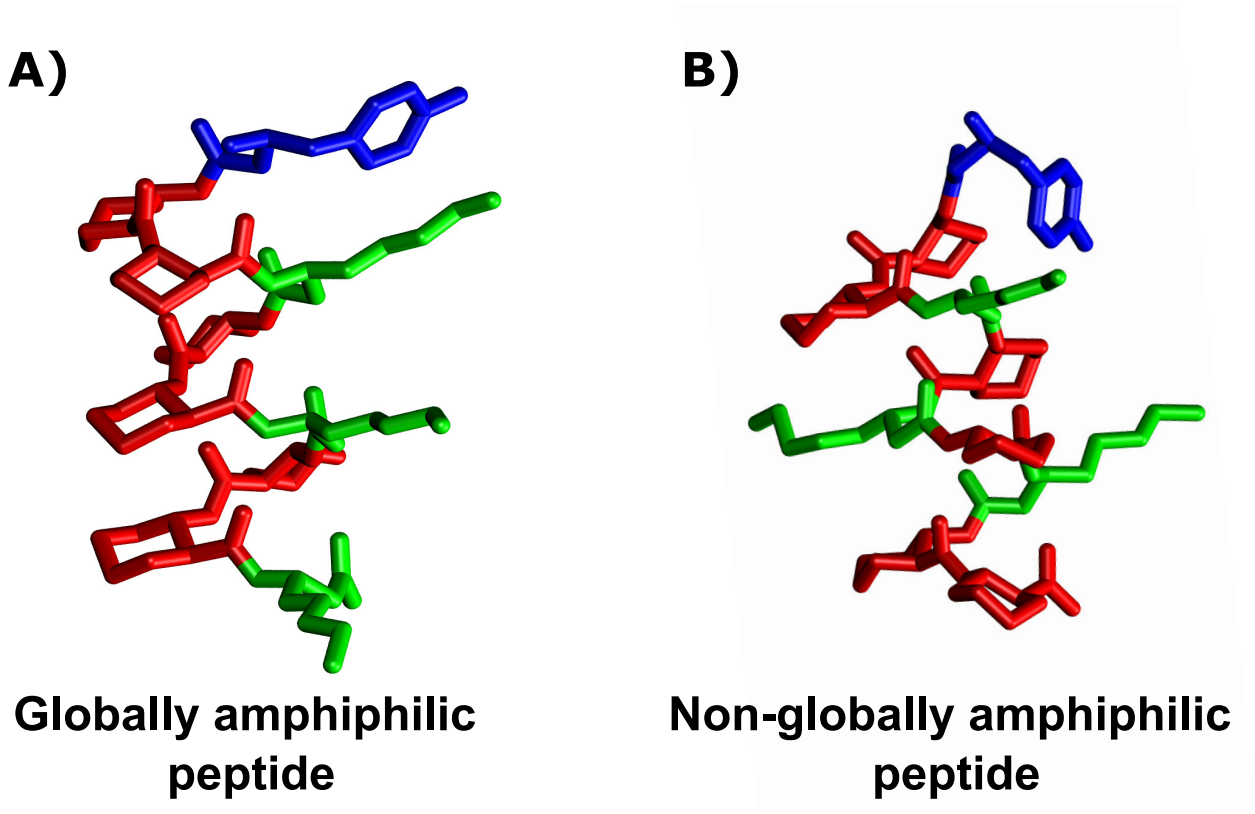

Figure 1: Three-dimensional representation of the β-peptides of our interest ('AAK'). A: Globally amphiphilic (GA) and B) non-globally amphiphilic (non-GA) isomers of AAK. The β-peptide is shown in licorice representation with hydrophobic ACHC residues in red, β-lysine groups in green and β-tyrosines are in blue.

rally occurring antimicrobial peptides such as magainin, melittin or LL37. More importantly, Gellman and coworkers[12] have explored the interplay of sequence-specificity and the antimicrobial activity in AAK. Specifically, the design of a sequence-arrangement of AAK in which the hydrophobic ACHC and hydrophilic β-homolysine residues are globally segregated, gave rise to a globally amphiphilic (hereby called 'GA' isomer) sequence isomer (see Figure 1A)). Experimental investigations led by Gellman and coworkers[12] have previously shown that the GA isomer of AAK can impart strong anti-bacterial activity on both gram-positive and gram-negative bacteria at a very low minimum inhibitory concentration (MIC). Specifically, the GA isomer of AAK was found to be comparable or more potent than the established antimicrobial natural peptides and was also found to be less hemolytic than the natural antimicrobial peptides.[5] The trends were similar for the anti-fungal activity of GA isomer of AAK on *Candida albicans*[15] with MIC value ranging between 16-32 μg/ml. AAK was also found to induce leakage of enzyme β-galactosidase from *Bacillus subtilis*,[13] thereby suggesting membrane permeabilization by β-peptides. On a related study, Gellman group also had investigated the role of amphiphilicity in the antimicrobial activity of AAK by synthetically designing a non-globally amphiphilic sequence-isomer of AAK (hereby called 'non GA' isomer of AAK) via evenly distributing single hydrophilic β-homolysine residue on all faces of 14-helical AAK. It was found that the antimicrobial potency of non GA isomer is significantly low, in contrast to its potent counterpart.[12,15] These observations suggested that the antimicrobial activity of AAK is strongly sequence-dependent, with GA isomer of AAK showing strong antibacterial and antifungal propensity than its non GA counterpart. Nonetheless, while these experimental investigations provide convincing macroscopic evidence of antimicrobial activity of AAK and the associated sequence-dependence, to the best of our knowledge, a molecular-level insight towards plausible mechanism of the antimicrobial activity of this 'short-chain' β-peptide, in comparison to natural antimicrobial peptides, has remained unexplored.

Since the origin of antimicrobial peptides' activity is believed to be rooted in their inter-

action with the membrane of the bacteria,[17] we wanted to explore how a membrane environment would respond to exposure to a growingly increasing concentration of β-peptides. In this current work, the pertinent question we ask: What is the plausible mechanism of membrane-disruption ability by these AAK ? Multiple hypotheses exist[1–3] in general to describe the principle steps leading to the membrane-disruption by antimicrobial peptides. Central to all prevailing hypotheses is the possibility of trans-membrane pore formation by antimicrobial peptides.[18,19] Does it form any transmembrane water channel? Or does it disrupt the membrane integrity in so-called "carpet like"[3,4] mechanism? In fact, natural antimicrobial peptides namely magainin-H2, melittin are believed to form trans-membrane pore across the membrane bilayer.[20,21] However, it is also believed that in general, there is no unique mechanism and it strongly depends on the specific antimicrobial peptides of interest.[22,23] The question of membrane-disruption mechanism is even more relevant for AAK mainly due to the significantly distinct molecular architecture and *short* sequence lengths of these rigid β-peptides compared to its flexible and sequentially long large molecular weights natural counterparts like magainin-H2 and melittin.

In the current work, we address these questions via coarse-grained molecular dynamics (MD) simulations of interactions of GA and non GA isomers AAK with a mixed 3:1 bilayer of 1-palmitoyl-3-oleoyl-sn-glycero-2-phosphoethanolamine (POPE) and 1-palmitoyl-2-oleoyl-sn-glycero-3-phosphoglycerol (POPG) lipids, a model bacterial-mimicking membrane.[24–26] We systematically develop a coarse-grained model for both sequence-isomers of the β-peptide within the frame-work of popular MARTINI model. The developed coarse-grained model, in combination with MARTINI membrane[27] and MARTINI polarisable coarse-grained water,[28] enabled us to investigate longer time-scale event involving membrane-β-peptide interaction. Interestingly, in these ultra-long coarse-grained MD simulations involving multiple copies of GA isomers of AAK and membrane, we observed spontaneous formation of peptide-induced transmembrane pore and water leakage inside the hydrophobic core, leading to disruption of membrane integrity. Analysis based on the tilt angle and end-to-end distance

of the of the pore-forming β-peptides suggested that these short-chain biomimetic peptides are able to form trans-membrane pore by stretching themselves across the membrane in a tilted manner. Finally, the pore forming ability by β-peptides was found to be sequence-dependent, with the non GA isomers, at similar P/L ratio, not being able to disrupt the membrane integrity. Taken together, the investigation elucidated a comprehensive mechanism of membrane-disruption by short-chain synthetic biomimetic peptides and identified water-filled pore formation as a key event.

Results and Discussions

An optimised model for membrane-β-peptide interaction:

To access relatively longer time scale event of interaction between membrane and our biomimetic peptide of interest β-peptide, we employed a coarse-grained framework based on MARTINI force field.[27,29–32] In this work, a mixed composition of phospholipid bilayer of POPE and POPG at 3:1 ratio has been chosen due to its past consideration as a mimic for bacterial membrane.[24–26] Additionally, β-peptides also have been previously investigated for its membrane activity in experimental assays solely involving model phospholipid bilayers or large unilamelar vesicle.[33] The lipid bilayer composition was modelled using MARTINI lipid force field. The choice of coarse-grained model allowed us to use relatively wider lipid bilayer (see table 1) than that typically employed in all-atom simulations. We employed polarisable MARTINI water model[28] for coarse-grained MARTINI force field for simulating the aqueous phase of the lipid bilayers. The choice was due to its superior ability to reproduce the water dielectric property, orientational polarizibilities and membrane interfacial electrostatic property more faithfully than the regular MARTINI water model. Accordingly, the Martini lipid and protein force fields compatible with MARTINI polarizable water were chosen in the current work. As detailed later, we would find that the usage of polarisable MARTINI water[28] (in contrast to regular MARTINI coarse-grained water[27]) was instrumental in ob-

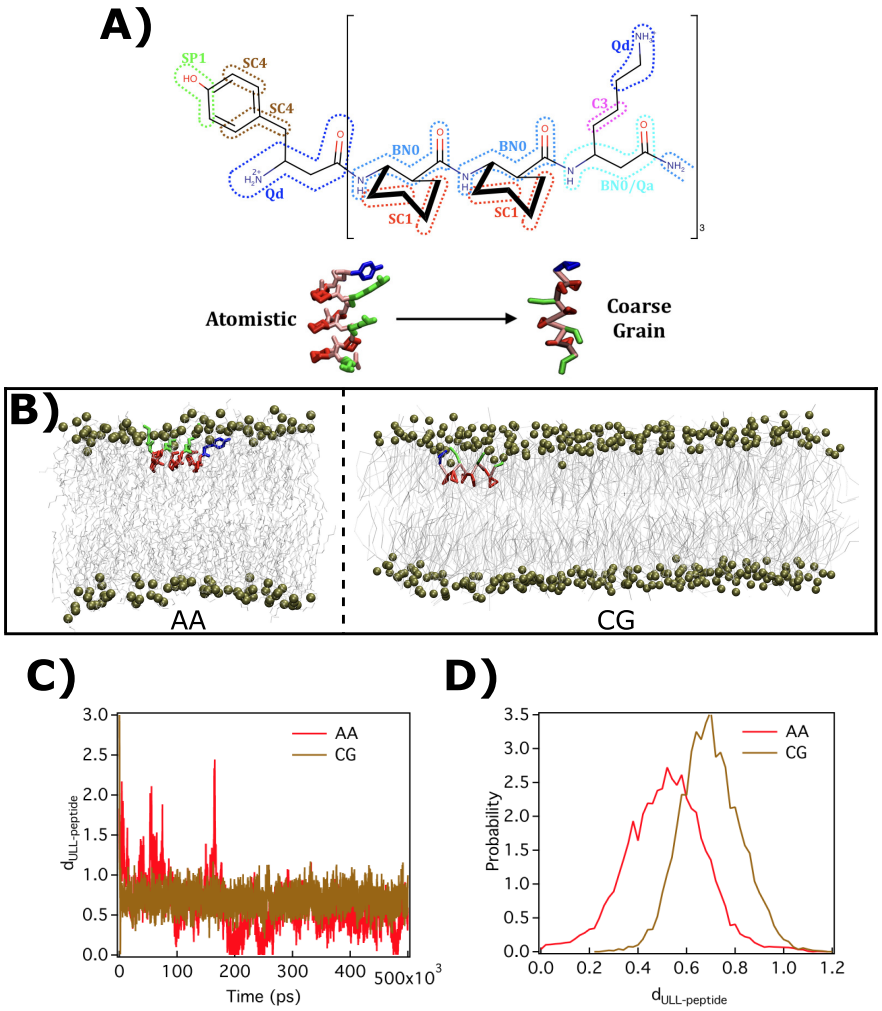

Figure 2: A. Mapping of β-peptides to MARTINI based coarse-grained Model. Bottom: Shown also snapshot of all-atom and coarse-grained counterpart. B. Snapshot of equilibrated configuration of single copy of GA in membrane interface as obtained from all-atom simulation and coarse-grained simulation. C. Comparison of time-profile and D. probability distribution of peptide-membrane distance (along z) at P/L 1:128 between all-atom and coarse-grained simulations

serving peptide induced trans-membrane pore in long time scale simulations. Due to the difference in the nature of backbone frame-work between naturally occurring α-amino acid and synthetically designed β-amino acid, the project prompted us to design coarse-grained model of GA and non GA isomer of AAK. As detailed in the method section, we developed a MARTINI-compatible coarse-grained model for the 10-residue β-peptide AAK, by iterative optimisation against all-atom simulation trajectory. Figure 2A provides the coarse-grained mapping scheme employed in the current work for GA isomer of the β-peptide.

Both in vitro and in vivo investigations into the anti-fungal and antibacterial abilities of sequence-isomers of β-peptide of our interest, AAK, have shown that it kills pathogen cells at a much lower concentration than many naturally occurring antimicrobial peptides. Towards this end, we first explored how the membrane/β-peptide interaction behaviour at a *single peptide level*, simulated using coarse-grained frame-work, would compare against those performed using an atomically detailed force field. We individually simulated the interaction of single copy of GA isomer of AAK, initially present in aqueous media, with a 3:1 POPE/POPG phospholipid bilayer, in an all-atom and coarse-grained representation. We find that, in both all-atom and coarse-grained simulations, single copy of AAK, starting from aqueous media, gradually approaches the hydrophilic interface of the phospholipid bilayer and eventually gets partitioned in the inner membrane interface. Representative snapshots in figure 2B provide a pictorial view of the eventual membrane-adsorbed state of GA isomer of AAK at single peptide level, obtained from all-atom and coarse-grained model. The comparison indicates qualitatively a very similar membrane-adsorbed state obtained in both types of simulations at single peptide level. The time profile and distribution of centre of mass distance (figure 2 C-D) between GA isomer and phosphate atoms of proximal leaflet also compares very well in both all-atom and coarse-grained simulations. Together, these observations validate that the coarse-grained model is able to qualitatively capture the basic membrane-adsorption feature of amphiphilic β-peptide and compare well against a similar simulation performed using more detailed model. Moreover, at high peptide concentration,

we find that at short-time scale, the present coarse-grained model reproduces very similar early-stage behaviour of membrane/β-peptide interaction, as found in 1 μs-long all-atom simulation of membrane interactions with multiple copies of β-peptides: In both cases (see first two rows of figure 3 for coarse-grained simulation and figure S2 for all-atom simulation) the β-peptides undergo spontaneous self-aggregation and membrane-adsorption within a 1 μs long simulation. These initial benchmark assessments of the coarse-grained model provided early promises for employing them in long time scale investigations.

Table 1: Details of the systems for simulation using GA isomer of AAK using MARTINI model. All β-peptide copies were initially placed in aqueous phase close to one side of the membrane. Each system was charge-neutralised by adding necessary counter ions.

System	Number of water	P/L ratio	Simulation Time(μs) $\times$ number of replica
β-peptide-less bilayer	6538	0	5 μs $\times$ 2
1 GA in 388 lipid	7761	1:388	20 μs $\times$ 2
5 GA in 336 lipid	6461	1:67	40 μs $\times$ 4
10 GA in 388 lipid	10010	1:39	20 μs $\times$ 4
15 GA in 336 lipid	8324	1:22	20 μs $\times$ 4

Simulations capture spontaneous transmembrane pore formation by short-chain β-peptides

Encouraged by the observation of efficient membrane-adsorption GA isomer of AAK towards membrane interaction manifested at single β-peptide level in a coarse-grained model, we explored the effect of high concentrations of GA isomer on the membrane. As enumerated in table 1, in our coarse-grained simulation, we systematically varied the P/L ratios within a wide range of 1:388 to 1:22 to investigate the interaction of increasing concentration of β-peptides with the membrane. At a very low P/L ratio of 1:388, which involved interaction of single copy of AAK with the membrane, as described earlier, the β-peptide approached the

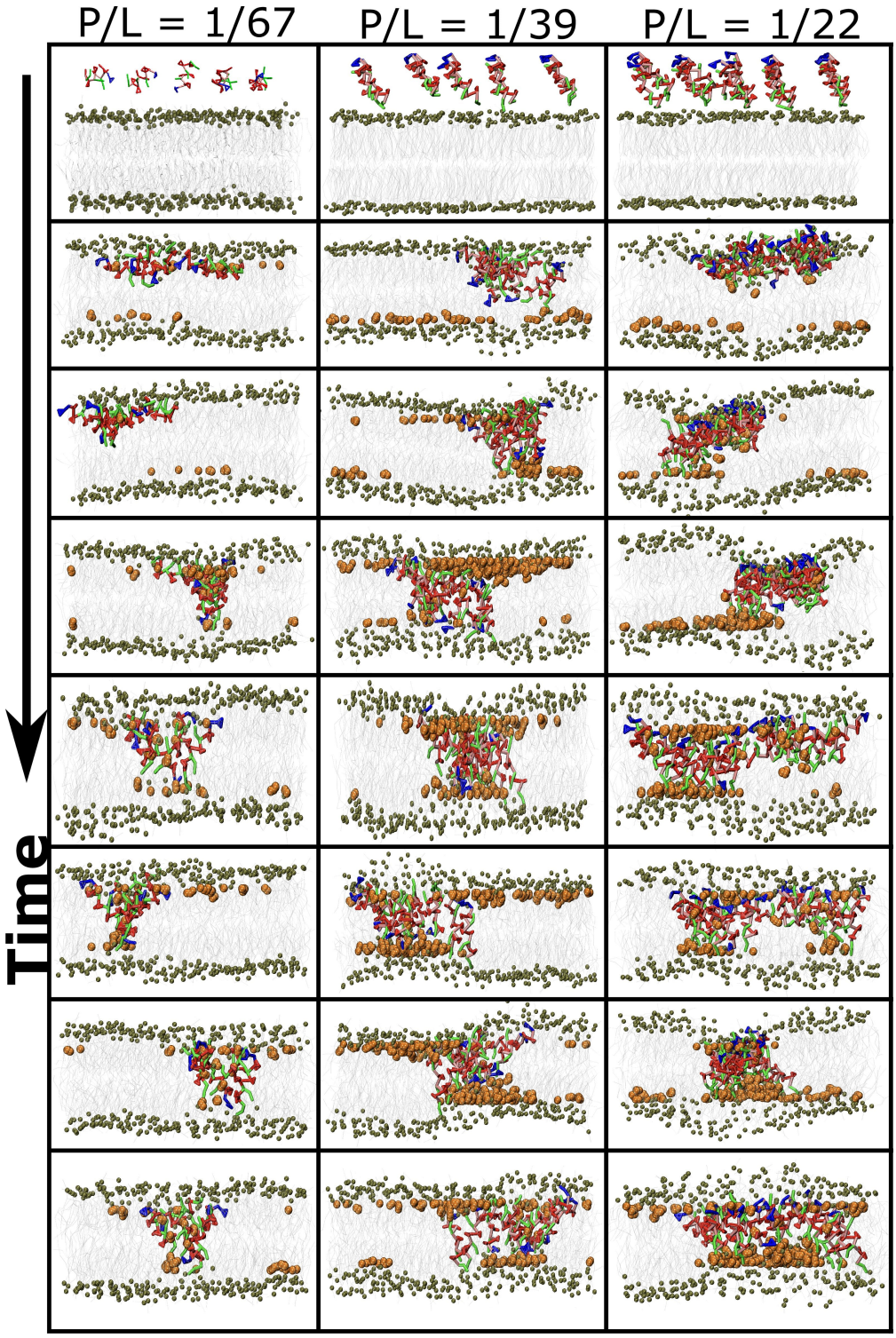

Figure 3: Time profile of account of β-peptides/membrane interaction at diverse P/L ratios. As a general trend, the β-peptides, after initiating from aqueous media, gradually assembles and partitions into the membrane interface. This is followed by transmembrane insertion of a number of β-peptide copies inside the membrane. The β-peptides eventually span across both the bilayer. Color code: TAN : Phosphate groups of lipids, ORANGE : Polarized water, BLUE :: Tyrosin, GREEN : Lysin, RED : ACHC residues.

membrane interface of the proximal leaflet and remained partitioned across the membrane interface. However, intriguingly, at a threshold P/L ratio of 1:67 (containing 5 peptides and 336 lipid molecules), coarse-grained simulations at longer coarse-graining time scale up to 40 μs displayed that (see movie S1 and left column of figure 3 for a visual account of process) few copies of GA isomer of AAK, initially mutually well-separated in bulk water gets self-assembled and adsorbed on the membrane surface. The aggregates of β-peptides, upon being docked on the surface, act as a cage and displace a number of lipid head groups (see figure S3 A). The lipid displacement provides the required opening for favorable hydrophobic interaction between ACHC residues and the lipid tails and as a result the β-peptide copies got past the polar head group of the proximal leaflet of the membrane interface. The aggregation and organisation process of the β-peptides continue past the event of membrane-adsorption. Eventually, the peptide-aggregate, upon attachment to membrane interface, snorkelled past the membrane interface of proximal leaflet and got embedded in a transmembrane orientation and spanned across proximal and distal leaflets of the membrane. As seen in movie S1 and in left column of figure 3, the defects created due to peptide insertions across the membrane interface led to a number of water molecules getting leaked inside the membrane interiors, thereby giving rise to a transmembrane pore-like structure for maximising favourable contacts between lipid tails and the hydrophobic β-amino acid residues.

A cooperative pore formation process:

We systematically increased the P/L ratios to 1:39 and 1:22 by introducing additional copies of the GA isomers in the same side of water phase and performed series of individual MD simulations using coarse-grained model. Movie S2 and S3 demonstrate the event of the β-peptide/membrane interaction at the P/L ratios of 1:39 and 1:22. Figure 3 provides a visual account of membrane-peptide interaction at different time points of multi μs long trajectories at P/L ratios of 1:67, 1:39 and 1:22. In all these three P/L ratios, the trend of pore formation is generic, except that the event gets accelerated at higher P/L ratio. At P/L ratio of 1:22,

the formation of two distinct trans-membrane pores is also seen at an intermediate time point, which eventually coalesce into a single large pore. The pore formation event was found to be reproducible across multiple trajectories (2 out of 4 trajectories for P/L=1: 67 and 3 out of 4 trajectories for P/L=1:39 and 1:22 displayed stable pore formation. Each trajectory was 20-40 μs long.) As shown in figure S4, at lower than five peptide copy numbers and at a P/L ratio lower than 1:67, the peptides would only settle below the surface of bilayer causing a partial disruption. This indicates that pre-association of the peptides may increase pore propensity as shown experimentally in case of tetravalent magainin peptides.[34] Once the formation of transmembrane pore is completed, the pore remains stable for the rest of the period of simulation. On the basis of the observation that pore formation is facilitated by self-aggregation of β-peptides and a threshold P/L ratio is required for transmembrane pore formation, we conclude that this is a cooperative process. This is qualitatively consistent with past free energy based simulation result, albeit focussed on naturally occurring antimicrobial peptide melittin, that increasing the number of peptide copies reduces the barrier to pore formation.[35]

Quantifying and characterising the pore formation process

To characterise the extent of β-peptide insertion inside the membrane at a given P/L ratio, we compute the minimum distance (d_{min}) between individual peptide copies and the phosphate group of the distal leaflet of the membrane (see schematic in figure 4A). As shown in the figure 4A, for single peptide level, d_{min} remains stable at a value of 2.5 nm, which corresponds to the peptide remaining adsorbed in the membrane-interface of the proximal leaflet at a P/L of 1:388. However, at higher P/L ratios of 1:67, 1:39 and 1:22, we observe a sharp collective drop in the value of d_{min} from 2.5 nm to 0.5 nm for a number of peptide copies at a time scale of 5-10 μs in coarse-grained simulation, indicating the onset of translocation of a cluster of peptides inside the membrane interior and initiation of eventual transmembrane pore formation (left column of Figure 4). Interestingly for P/L ratio of 1:22, we observe

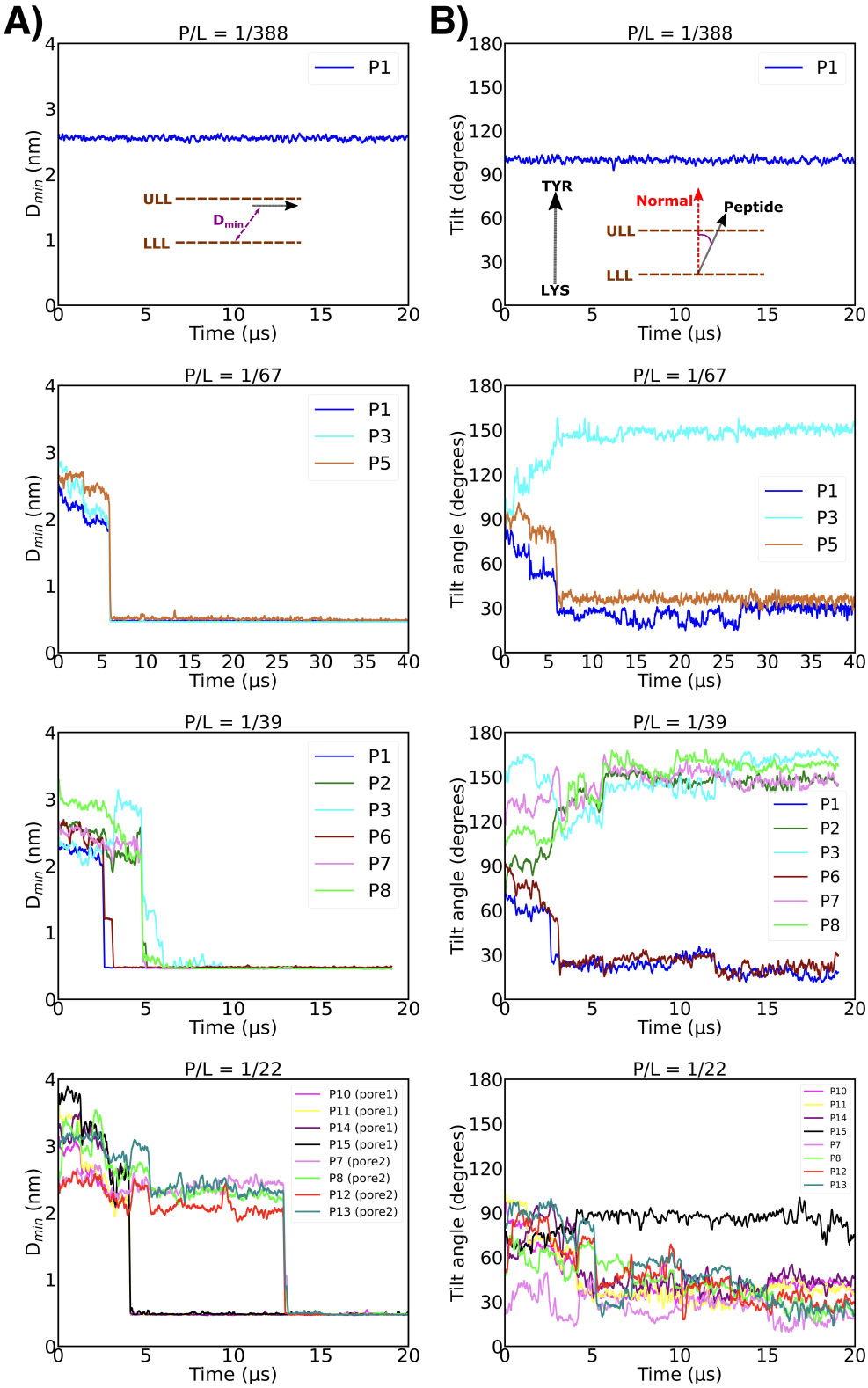

Figure 4: A. Comparison of time profile of extent of peptide insertions. Here, minimum distance between the phosphate group of distal leaflet and the peptide (d_{min}) has been considered as the metric. The sudden drop in the value of d_{min} signifies the onset of peptide translocation and pore formation. Only the time profile of pore-forming peptide has been shown. B. Comparison of time profile of tilt angle of the peptides with the membrane interface at diverse P/L ratios.

two such events in which d_{min} decreased for two independent peptide clusters, indicating the onsets of two distinct pore formations as confirmed by Movie S3 and of top panel of Figure 4A. Once the transmembrane pore formation is completed, the pore remains stable for the rest of the duration of 20 μs (40 μs for P/L ratio of 1:67) simulation.

Figures 4 B characterise the tilt angle between the β-peptide copy and the membrane surface normal. Based on this analysis, a tilt-angle of 90 degree would imply that the peptide is horizontally oriented with the membrane interface, which is the case for single peptide at P/L of 1:388. However, with increasing P/L ratio, we found that the β-peptides which formed the core of the pore, eventually transitioned from a tilt angle of 90 degree to a tilt angle closer to 30 degree or 150 degree (suggestive of reversal of peptide's orientation during membrane translocation), indicating that these pore-forming peptides have attained a transmembrane orientation. However, the tilt angle is not perfectly zero, suggesting a tilted orientation subtended by these pore-forming β-peptides with the membrane interface. Together, the analysis of time profile of tilt angle and d_{min} of the peptides indicate that the formation of transmembrane pore involves collective translocation of β-peptides at a multi-microsecond long time scale, in which this peptide eventually makes a tilted orientation with the membrane interface. The timescale required for the formation of pore containing minimum of five peptides (at a P/L ratio of 1:67) was around 8-9 μs in coarse-grained unit. As the P/L ratio and number of β-peptide copies increased to 1:39 and 1:22, the pore formation process and reorientation to transmembrane pose get expedited (2.5-5 μs). The reorientation of peptide from a surface to a transmembrane conformation is generally considered an important step in its pore-forming ability[36,37] and is believed to be associated with a considerable free energy barrier[38] . The observation of expedited transmembrane reorientation of β-peptides beyond a threshold P/L ratio qualitatively coincides with the previous report of reduced free energy barrier of reorientation of melittin with increasing P/L ratio.[38] Overall, similar analysis based on distance and tilt-angle also characterises transmembrane insertion of peptide clusters across multiple trajectories (see Figure S5 and

S6 for P/L ratio of 1:39 and 1:22)

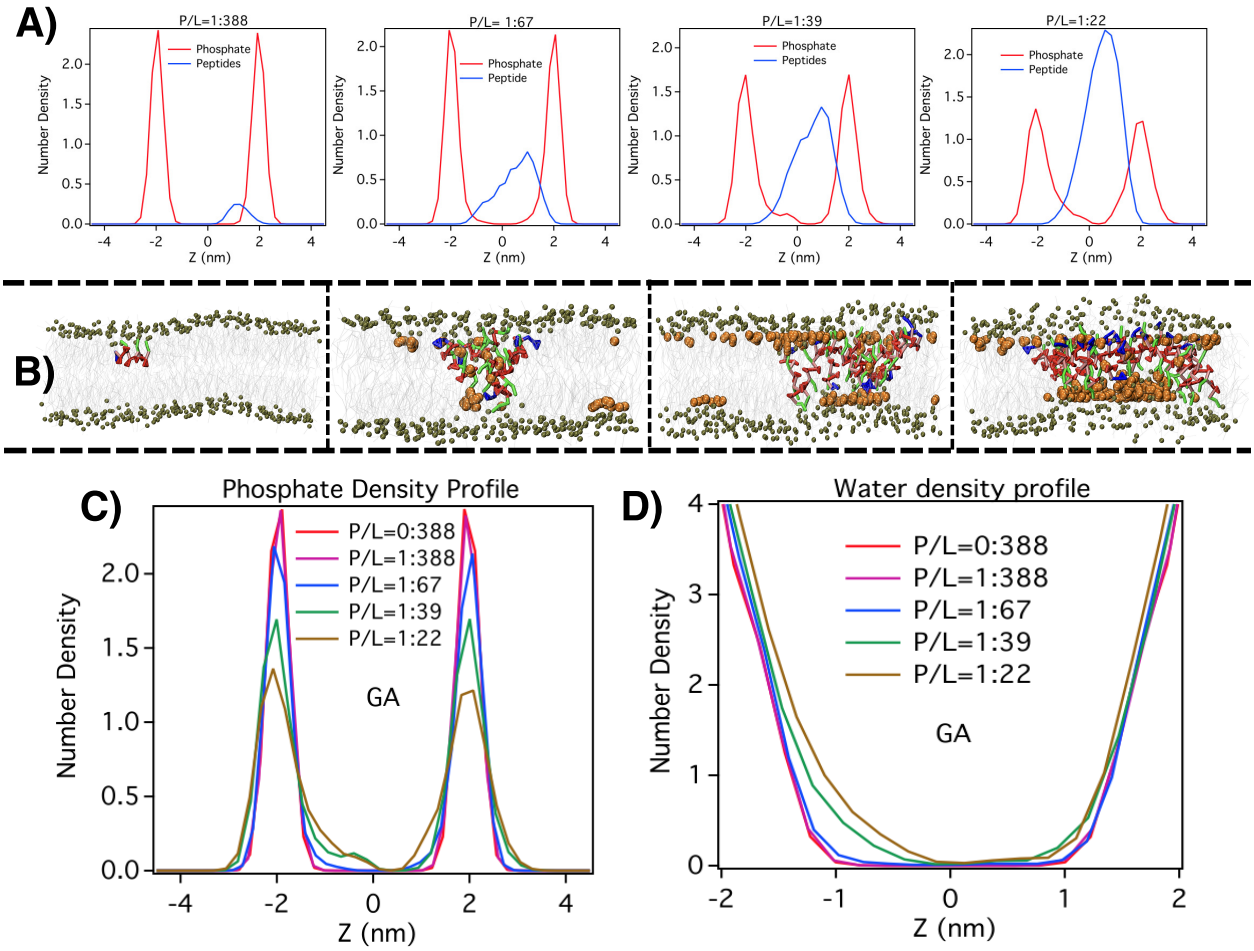

Figure 5: A. Density profile of GA peptides across membrane interface at multiple P/L ratios. B. shown are the representative snapshots of equilibrium conformation in all P/L ratio. C-D: Density profile of phosphate and waters at multiple P/L ratios.

Figure 5A compares the peptide density profiles along the surface normal for all P/L ratios investigated here. These density profiles were averaged over last 3 μs duration of the simulation (see snapshot in figure 5B). Consistent with previous section's description, with increasing P/L ratio, we find that the β-peptide density past the phosphate group gradually increases inside the hydrophobic core of the membrane and eventually the tail of the density profile stretches upto distal leaflet of the membrane at high P/L ratio, implying that the peptides span both the leaflets and form a transmembrane channel. Figure S4 indicates that β-tyrosine residue mostly remains localised close to the membrane interface while the

hydrophobic ACHC groups span the core of the transmembrane pore. The density of the phosphate groups (figure 5C) also increases inside the hydrophobic core of the membrane with increasing P/L. The sharp phosphate density profile in neat membrane gets gradually smeared with increasing P/L ratio. Most importantly, as is observed in the water density profile (see figure 5C), the peptide-membrane interaction leads to considerable increase in water density inside the hydrophobic core of the membrane with increasing P/L ratio. The representative snapshots at high P/L ratios of 1:39 and 1:22 especially depict (figure 5B) the presence of a distinct layer of water near the inner part of the both the leaflets. This suggests that these transmembrane pores are wet in nature and we believe that these interfacial waters help maintain the transmembrane pore via favourable interactions with the polar terminal residues of AAK.

There are diverse proposals of variants of trans-membrane pores including barrel-stave, toroidal and carpet types. The detailed characterisation of the pore showed that β-peptides induce local defects in the bilayer and subsequently the head groups of the lipids line the pore together along with the peptides. The visual inspection of the pore also revealed that the peptides are unevenly distributed i.e. higher concentration of peptides were present in the upper leaflet in comparison to the ones in lower leaflet. The tilt-angle analysis of the pore-forming peptides (discussed in the previous paragraph) indicates that the β-peptide aggregate gets inserted almost vertically into the membrane, almost baring the characteristics of a barrel stave pore. However, the pore is not perfectly cylindrical, rather it subtends a non-zero angle with the membrane normal. Additionally, the snapshots of the pore also shows minor line-up of the displaced lipid head groups. However, the lining of lipid head-groups is not as prominent as what would be observed in an ideal toroidal pore.

Finally, we stress that the choice of polarizable MARTINI coarse-grained water[28] for modelling solvent was instrumental in observation of the pore in the current simulations. The usage of regular Martini coarse-grained LJ water model only resulted in the peptide adsorption on the membrane leaflet and did not lead to any pore formation. (see figure

S7) This suggests the importance of appropriate representation of the membrane interfacial electrostatics via choice of better water model.

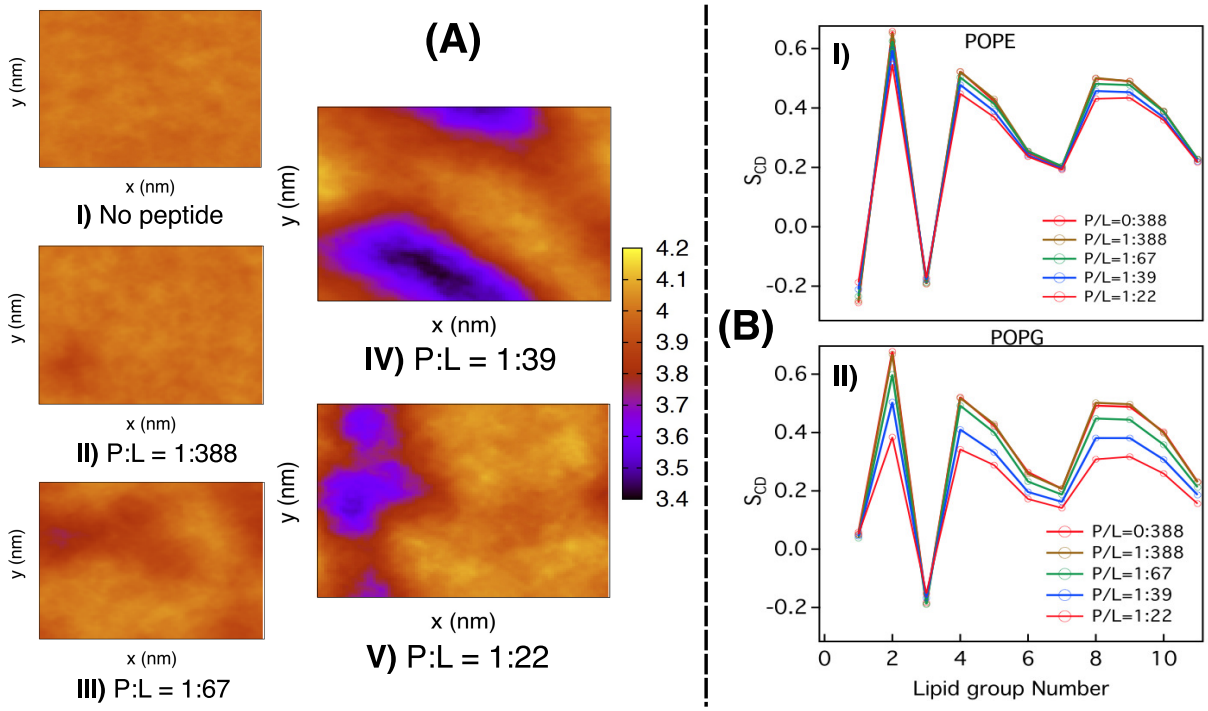

Figure 6: Comparison of A. Bilayer thickness profile B. Lipid order parameter of the POPE and POPG lipids across multiple P/L ratios of GA isomer

We find that the impact of pore formation and water leakage on the overall membrane integrity is mostly local. This is demonstrated in the two-dimensional bilayer thickness profiles (figure 6) at diverse P/L ratios. Within P/L ratio of 1:388 to 1:67, the bilayer thickness profile remains uniform, similar to that in peptide-less membrane. However, at higher P/L ratio of 1:39, we find localised non-uniformity in the membrane-thickness profile, which eventually grows at P/L ratio of 1:22. As an indication of disrupted membrane integrity induced by GA isomer of β-peptide, the deuterium order parameters of the POPG lipid tails systematically decrease with increasing P/L ratio. Interestingly, the order parameter of POPE lipid does not change in presence of peptides, indicating specific interaction between POPG lipids and β-peptide.

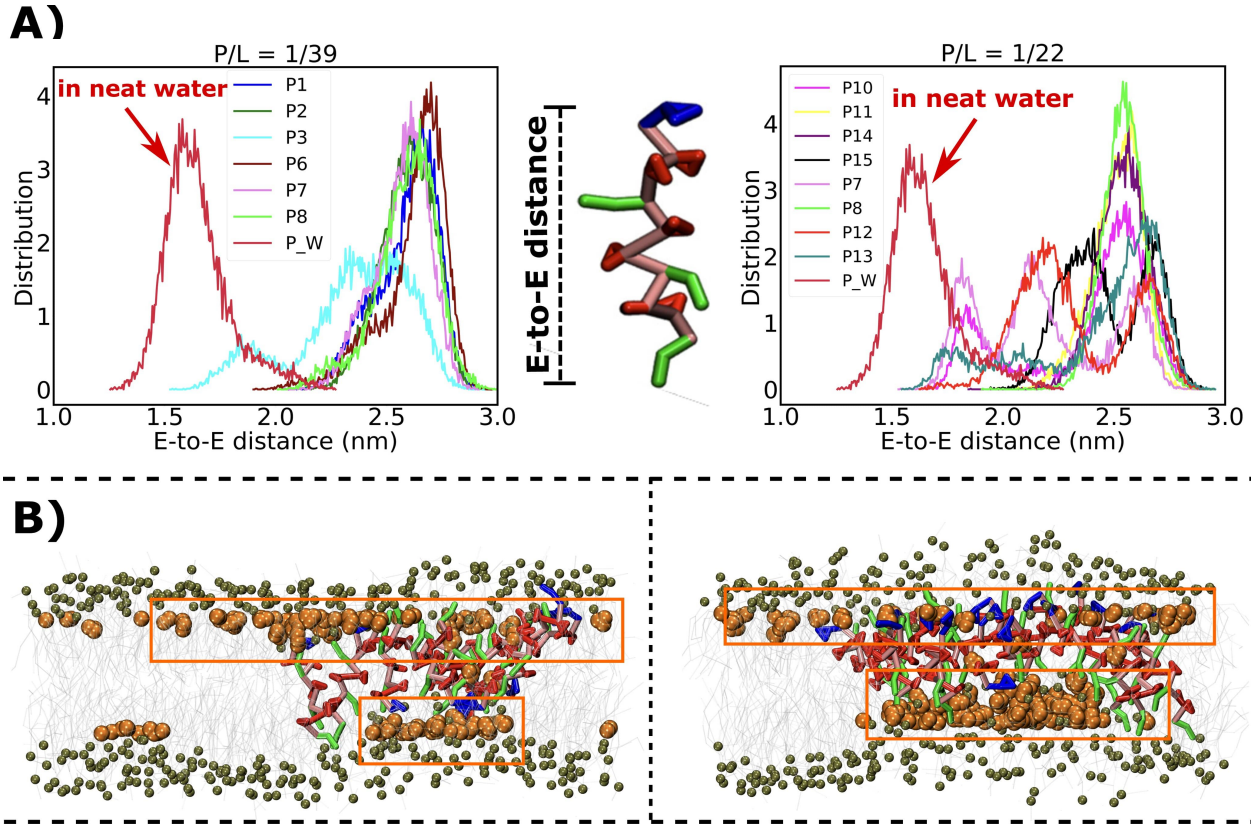

Figure 7: A. Comparison of the probability distribution of GA isomer's end-to-end distance between that in neat water and that inside membrane at multiple P/L ratio B. The representative snapshot of pore showing water-layer anchoring the transmembrane pores.

Reconciling short-chain architecture of β-peptides and its trans-membrane pore formation ability:

A distinct feature of the β-peptide of current interest i.e. GA isomer of AAK is their relatively shorter architecture (only 10-residue) than typical natural antimicrobial peptides such as magainin (23 residues), melittin (27 residues) or LL37 (37 residues). A pertinent question is: how are these short-length β-peptides able to form membrane-spanning pore in the bilayer? Towards this end, we analyse the end-to-end distance of the β-peptide in different media. Figure 7 A compares the distribution of end-to-end distance of this specific β-peptide. We find that in bulk water, the average end-to-end distance is approximately 1.5 nm, which remains almost similar in the case where single peptide remains adsorbed in the membrane/water interface (i.e. at P/L = 1:388). However, at higher P/L ratios, we note that the end-to-end distance of individual transmembrane peptides, which are constituent of the pore, increases to approximately 2.5 nm over time.(figure 7 A) A careful inspection of time profile of the end-to-end distance in figure S8 suggests that the onset of increase in the pore-forming β-peptides' end-to-end distance coincides with the onset of transmembrane pore formation of the β-peptides inside the membrane. The extended chain length of these peptides inside the membrane interior enable them to span the membrane and form trans-membrane pore. A plausible rationale for these observed extension of these pore-forming peptides is that, once inside the hydrophobic core of the membrane, the polar N-terminal residue β-tyrosine or hydrophilic C-terminal residue β-lysine residue of these β-peptides aim to reach out to the polar head groups of the distal leaflet for favourable interaction (see figure S3 B), which leads to a possible elongation of these peptides. Although, the transmembrane β-peptides are stretched inside the bilayer, it is still shorter than average membrane thickness of the neat POPE/POPG bilayer. A visual inspection of the transmembrane pore and analysis of bilayer thickness profiles at high P/L ratios of 1:39 and 1:22 (Figure 7 B) shows that the bilayer becomes non-uniform in presence of these β-peptides and undergoes localised thinning, which helps these extended pore-forming β-peptides to span the leaflet. Finally,

as discussed earlier, the presence of layer of interfacial water acts (figure 7 B) as additional cushion to support the transmembrane pore.

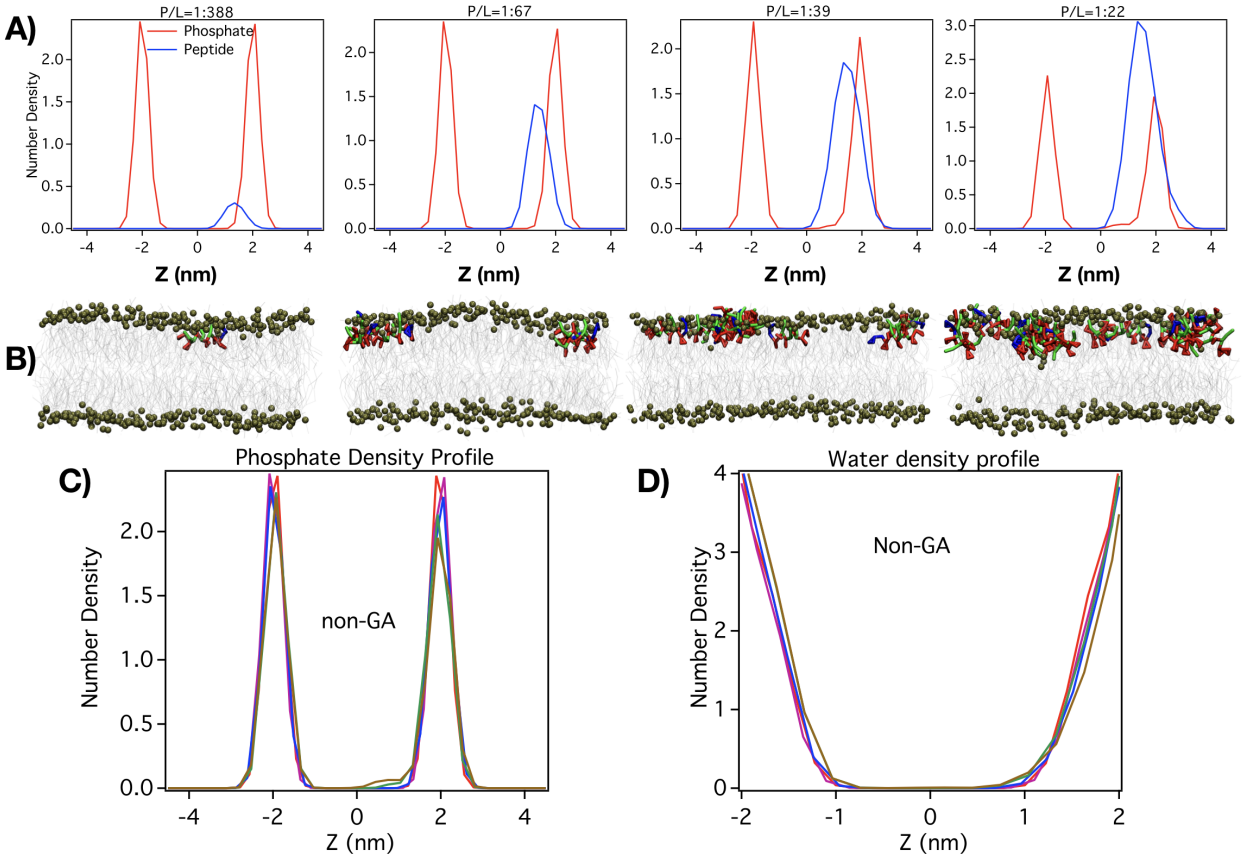

Figure 8: A. Density profile of non-GA isomers across membrane interface at multiple P/L ratios. B. Representative snapshots of non-GA isomers interacting with membrane at all P/L ratios C. Comparison of phosphate density profiles in presence of non-GA isomers at diverse P/L ratios. D. Comparison of water density profiles in presence of non-GA isomers at diverse P/L ratios.

The pore formation ability is sequence-selective:

We investigated whether the pore forming propensity of β-peptides is sequence dependent. Accordingly, we also simulated the interaction of non GA isomers of AAK with the membrane at a wide range of P/L ratio, similar to GA isomer. The peptide density profiles of non GA isomers are compared in figure 8A across P/L ratios ranging between 1:388 to 1:22. We

find that, unlike GA isomer, the peptide density profile does not span across both the leaflets in non GA isomer even in the highest P/L ratio of 1:22. Instead, as shown by the representative snapshot in figure 8B, we see that the β-peptide copies in non GA isomer self-assemble into small isolated oligomeric cluster and remain adsorbed on the membrane interface, without showing any tendency of translocation inside the membrane interior. This is also reflected in unchanged phosphate density profiles and water density profiles in the membranes across entire range of P/L ratio involving non GA isomers (figure 8C-D). Finally, relatively unchanged bilayer thickness profiles (figure 9 A) and deuterium order parameters (figure 9B) across P/L ratios in case of non GA isomer relative to GA isomer clearly suggests that non GA isomer of AAK would not be able to disrupt the membrane integrity unlike GA isomer at similar P/L ratio. These results clearly suggest that the presence of global segregation of hydrophilic and hydrophobic residues in a β-peptide, as in GA isomer, is key to its ability to form water-lined transmembrane pore and to disrupt membrane integrity.

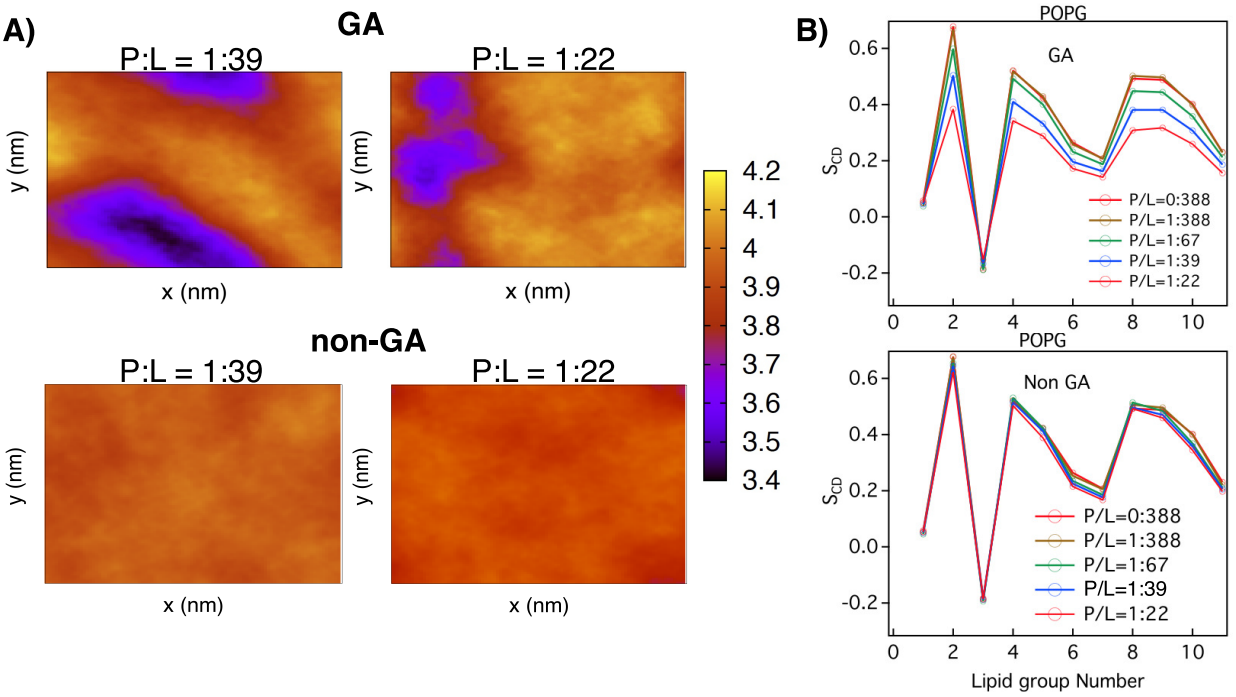

Figure 9: A. Comparison of bilayer thickness profile between GA and non GA isomers of AAK at two P/L ratios. B. Comparison of POPG lipid order parameter between GA and non GA isomers .

Conclusion

Unravelling the mechanistic action of antimicrobial agents at an atomistic resolution has always been a key desirable from both experimental and computational perspectives. Specifically, it remains more intriguing to decipher the membrane-disrupting mechanism for amphiphilic biomimetic peptides which manifest strong antimicrobial properties despite being much shorter in chain-length and lower molecular weight than their natural counterparts. In this work, via computer simulation using coarse-grained model, we have elucidated key mechanisms of membrane-disruption process of a set of isomers of a β-peptide, AAK, which is known for their proven antimicrobial activity.

Our ultra-long coarse-grained simulations involving systematically developed coarse-grained model for AAKs, in combination with MARTINI lipid and polarisable water models, were able to capture the spontaneous membrane-disruption processes induced by short-chain β-peptide. As a key observation, beyond a threshold peptide/lipid ratio, these coarse-grained simulations revealed formation of spontaneous peptide-induced disordered pore and eventual water-leakage inside the membrane interior. These pores remained stable during the period of 20-40 μs-long coarse-grained trajectories. The pore forming peptides are not perfectly vertical with the membrane interface. Rather these peptides showed a non-zero tilt angle with the membrane interface. Interestingly, the pore-forming peptides were found to be considerably extended inside the membrane interior in a ploy for the polar residues to reach out to the headgroups of the distal leaflet. The pore formation propensity increased with increasing P/L ratio, with eventual observation of multiple pores at high P/L ratio. The β-peptide-induced pore formation also led to increasing non-uniformity in membrane thickness and disordered lipid tail. Finally, similar computer simulation using a non globally amphiphilic isomer of the same β peptide neither led to any transmembrane pore formation nor induced any water leakage inside the membrane core, which explained its experimentally proven non-potency in antimicrobial activity. We also note that the coarse-grained model used in the current work i.e. MARTINI forcefield together with MARTINI polarisable water

is not devoid of criticism and has recently been reported[39] for discrepancy in representing the membrane-adsorption process by nanoparticle. However, the ability of the currently presented coarse-grained model in recovering all-atom simulation results of early stages of peptide-membrane interaction provides confidence for following its long time scale behaviour. The observation of pore formation in this current coarse-grained simulation is consistent with a previous biochemical investigation of Epand and coworkers[33] in which, a pair of different but closely related 14-helical β-peptides were probed for their interaction with model membranes. Using an assay involving large unilamelar vesicles this work had indicated leakage and possibility pore formation and lipid flip-flop by this class of β-peptides. The current work provides convincing evidence in support of pore formation by a related but more potent antimicrobial β-peptide AAK and brings out the associated molecular mechanism of the full process.

As a major advancement, this work highlights key perspectives of membrane-activity of synthetic biomimetic oligomers. Going beyond precedent computer simulation studies, which have explored mainly membrane-attachment of peptides at a low Peptide/Lipid ratio or which have started with manually preformed specific transmembrane pore,[22,23,40] our current work takes a step forward and captures the complete process of membrane-disruption via spontaneous formation of barrel-stave pore. The thermodynamic feasibility of membrane disruption via spontaneous pore formation by these rigid 10-residue-long β-peptide foldamers were also validated in a wide range of P/L ratios. The superior ability of imparting antimicrobial activity by AAK at a lower MIC than the natural antimicrobial peptides has previously been stressed by Gellman and coworkers. In this regard, the observation of transmembrane pore formation via these short-chain peptides and the possibility of chain extension to reach out to the distal leaflet are interesting phenomena. More over the ability to induce trans-membrane pore by AAK at a threshold P/L ratio of 1:67, as found in the current simulation, at considerably lower concentration also speaks of potent membrane-disrupting ability by these β-peptides. As we have emphasised earlier in the article, choice of polarisable

MARTINI coarse-grained water[28] (in contrast to regular uncharged MARTINI water[27]) was instrumental in capturing the pore formation process by these β-peptides, which suggests proper role of water model in capturing the process. The requirement of presence of multiple copies of β-peptides for pore formation is a suggestive of cooperative process. In addition, the observation that the reorientation of β-peptides from surface-bound state to transmembrane state is facilitated beyond threshold P/L ratios, opens up future direction for systematic quantification via free energy based characterisation of pore formation process[35,37,38] using suitable collective variable.[41]

The membrane disruption process by antimicrobial agent via pore formation is considered to be a slow process,[36,37,42] the time scale of which is not often prohibitive via all-atom simulation. For example, a 5 μs long all-atom simulation of 10 surface-bound antimicrobial peptides alamethicine did not show any spontaneous membrane insertion.[22] To accelerate insertion of the peptides, the temperature had to be artificially raised to very high temperature and external electric field needed to be employed. In this regard, the current work's implementation of coarse-grained model in combination with Martini polarisable water is a practical way-forward and more insights can potentially be further harnessed via a resolution-switch to an all-atom model.[43] The investigation reported here opens up multitudes of opportunities towards understanding of the mechanistic aspects of the membrane-disruption capability by both natural and biomimetic macromolecules across multiple membrane compositions. Recent works by Gellman and coworkers on exploring random copolymeric biomimetic peptides as cost-effective and efficient antimicrobial agents are being seen as major paradigm shifts.[44–46] These works suggest a departure from the preconceived notion of requirement of secondary structure as a key pre-requisite for the manifestation of antimicrobial activity and open up possibilities of venturing into atomistic view of these random copolymeric antimicrobial agents.

Method and model

Development of coarse-grained model for β-peptide:

Due to the difference in the nature of backbone frame-work between α and β amino acid, the project required us to develop MARTINI-compatible model of GA and non GA isomer of AAK. Towards this end, we followed usual MARTINI protocol for parameterising a new molecule, in this case a 10-residue β-peptide. Accordingly, we first performed benchmark all-atom simulation of single copy of AAK in bulk water and the simulation trajectories served as the reference. The CHARMM forcefield of β-peptides, earlier developed by Zhu et al.,[47,48] was employed here to model the β-peptides in all-atom representation. The water molecules are modelled by CHARMM-TIP3P water model[49] due to its compatibility with the parameters of lipid molecules. CHARMM[50] parameters are also used for the parameters of ions. Figure 2A represents the coarse-grained mapping scheme of GA isomer of AAK. The backbone of β-amino acid has one extra carbon atom than natural α-amino acid. Accordingly we used a five-to-one bead mapping for backbone of the β-amino acid. To mimic the effective size and hydrophobicity of 5:1 mapping (compared to usual MARTINI 4:1 mapping[27]), the nonbonding LJ parameters for backbone were increased to σ=0.50 nm (instead of MARTINI backbone value of 0.47 nm) and backbone ϵ values were increased to 125 percent of the MARTINI backbone values. Since both GA and non GA sequence-isomers of AAK are known to retain their rigid 14-helical conformations in membrane as well, similar MARTINI backbone nonbonding parameters for α-helix, were introduced as the atom types. The bond, angle and dihedral parameters of the backbone of AAK were then iteratively parameterised by performing iterative simulation of coarse-grained AAK in MARTINI polarisable water and comparing the distributions against the all-atom trajectories of the single chain of the β-peptide in water, till a best fit was obtained for respective distributions derived from all-atom simulations (see figure S1). The side chain parameters of βY and βK were directly adopted from analogous MARTINI side-chain parameters of their α-amino

acid counterparts[30] (compatible with MARTINI polarisable water), as the side chains in both cases are identical. Finally, the cyclic β-amino acid ACHC was coarse-grained via 3:1 mapping (usual MARTINI protocol for modelling cyclic functional group) and analogous MARTINI parameters of cyclohexane were adopted for side-chain of ACHC.

In order to determine the qualitative accuracy of the coarse-grained model developed for β-peptide, we first investigated, if at single peptide level, the coarse-grained model of GA isomer displays qualitatively similar membrane interaction as its atomistic counterpart . Accordingly we compared the adsorption ability of single-copy of GA isomer of AAK on POPE/POPG mixed bilayer in both all-atom and coarse-grained model. We found that the coarse-grained model was able to display spontaneous adsorption process of GA isomer of AAK on the membrane-interface, as is seen in all-atom simulation (figure 2B-D).

Long time scale peptide-membrane simulation using coarse-grained model:

Table 1 provides a summary of each of the coarse-grained MD simulations carried out with GA isomers of AAK in POPE/POPG lipid bilayers. A total of four separate systems was investigated, using a wide range of P/L ratio which involved 1-15 copies of GA isomer copies. In all CG simulations, we first mapped atomistic protein structure to the coarse-grained model using martinize.py script, appropriately modified for β-amino acid. Subsequently, we set up the POPE:POPG (3:1) bilayer along with its solvation by MARTINI polarised water by insane.py (http://www.cgmartini.nl/index.php/downloads/tools/239-insane). In all our systems of interest, simulations were initiated by placing all the β-peptide copies in the aqueous phase close to *one* of monolayers of the POPE:POPG (3:1) bilayer, with the empty space filled with martini polarised water ionized with a suitable amount of Na^+ and Cl^- martini ions to reach an electroneutral solution. The overlapping molecular contacts were initially removed by energy minimization using steepest descent algorithm. The asymmetric distribution of the peptides mimics the addition of peptide to a solution containing cells or liposomes, in which peptides adsorb to one monolayer only. Sufficient water layer was intro-

duced on the both side of the bilayer to ensure the β-peptide copies do not artificially reach to the other leaflet via periodic boundary condition. The production MD simulations were carried out for 20 μs. All production MD simulations were performed at 310.15 K, representing physiological temperature and 1 atmospheric pressure. The average temperature was maintained by velocity rescale temperature coupling scheme with membrane, proteins and water molecules individually coupled to thermal bath with a coupling constant of 1 ps. A semi isotropic pressure coupling approach was employed via Parrinello- Rahman scheme with a pressure coupling constant of 12 ps and isothermal compressibility of 1 bar^{-1}. Verlet cutoff scheme was employed for non bonded interaction with a cutoff for Lennard-Jones potential at 1.1 nm. The real space cutoff Coulomb potential was 1.1 nm with relative dielectric constant of 2.5 for polarized water. The long range electrostatic interaction was handled by reaction field, as per so-called MARTINI *New-RF*' recommendations[51] . All MD simulations were performed with the Gromacs 2018 simulation package,[52] together with GPU accelerations[51] A time step of 20 femtosecond was used and the neighbour list was updated every 10 steps. The simulation length for each trajectory at higher P/L ratios of 1:39 and 1:22 was 20 μs, while at P/L ratio of 1:67, the simulations were extended for 40 μs. For each P/L ratio, four independent simulation trajectories were spawned. A 5 μs-long control simulation with only POPE:POPG lipid bilayers containing 336 lipids (i.e. lacking any peptides) were also performed for comparison purpose.

For a systematic comparison, the entire simulation protocol and parameterisation was repeated for non GA sequence isomer as well . We refer to table S1 for system details for simulation using nonGA isomer. See figure S9 for the mapping scheme and optimised distributions.

For reference, we provide GROMACS-compatible topology and parameter files of GA and nonGA isomers of AAK along with an initial configuration of a single AAK in presence of membrane in the Supporting information.

Acknowledgments

This work was supported by computing resources obtained from shared facility of TIFR Center for Interdisciplinary Sciences, India. We acknowledge support of the Department of Atomic Energy, Government of India, under Project Identification No. RTI 4007. JM would like to acknowledge research grants received from Ramanujan Fellowship and core research grant provided by the Department of Science and Technology (DST) of India (CRG/2019/001219). PG would like to acknowledge the financial support by INSPIRE Faculty Grant (DST/INSPIRE/04/2015/002495) from DST of India.

Supporting Information

Supporting movies of pore formation process at P/L ratio of 1:67, 1:39 and 1:22. All gromacs formatted topology and parameter files along with sample configuration for both β-peptides investigated in the work (.zip) . All supporting figures referred in this manuscript are present in the supporting information.

References

(1) Zassloff, M. Antimicrobial peptides of multicellular organisms. *Nature* **2002**, *415*, 389.

(2) Borgden, K. Antimicrobial peptides: pore formers or metabolic inhibitors in bacteria? *Nature Rev. Microbiol.* **2005**, *3*, 238.

(3) Yeaman, M.; Yount, N. Mechanisms of antimicrobial peptide action and resistance. *Pharmacol.Rev.* **2003**, *55*, 27.

(4) Shai, Y.; Oren, Z. From "carpet" mechanism to de-novo designed diastereomeric cell-selective antimicrobial peptides. *Peptides* **2001**, *22*, 1629.

(5) Porter, E. A.; Wang, X.; Lee, H.; Weisblum, B.; Gellman, S. H. Non-haemolytic β-amino-acid oligomers. *Nature* **2000**, *404*, 565–565.

(6) Liu, D.; DeGrado, W. F. De Novo Design, Synthesis, and Characterization of Antimicrobial β-Peptides. *Journal of the American Chemical Society* **2001**, *123*, 7553–7559, PMID: 11480975.

(7) Chongsiriwatana, N. P.; Patch, J. A.; Czyzewski, A. M.; Dohm, M. T.; Ivankin, A.; Gidalevitz, D.; Zuckermann, R. N.; Barron, A. E. Peptoids that mimic the structure, function, and mechanism of helical antimicrobial peptides. *Proceedings of the National Academy of Sciences* **2008**, *105*, 2794–2799.

(8) Horne, W. S.; Boersma, M. D.; Windsor, M. A.; Gellman, S. H. Sequence-based design of alpha/beta-peptide foldamers that mimic BH3 domains. *Angew.Chem. Int. Ed.* **2008**, *47*, 2853–6.

(9) Frackenpohl, J.; Arvidsson, P. I.; Schreiber, J. V.; Seebach, D. The Outstanding Biological Stability of β- and γ-Peptides toward Proteolytic Enzymes: An In Vitro Investigation with Fifteen Peptidases. *ChemBioChem* **2001**, *2*, 445–455.

(10) Cheng, R. P.; Gellman, S. H.; Degrado, W. F. β-Peptides: From Structure to Function. *Chem. Rev.* **2001**, *101*, 3219.

(11) Gellman, S. H. Foldamers: A Manifesto. *Acc. Chem. Res.* **1998**, *31*, 173.

(12) Raguse, T. L.; Porter, E. A.; Gellman, S. H. Structure-Activity Studies of 14-Helical Antimicrobial β-Peptides:? Probing the Relationship between Conformational Stability and Antimicrobial Potency. *J. Am. Chem. Soc.* **2002**, *124*, 12774.

(13) Porter, E. A.; Weisblum, B.; Gellman, S. H. Mimicry of Host-Defense Peptides by Unnatural Oligomers:? Antimicrobial β-Peptides. *J. Am. Chem. Soc.* **2002**, *124*, 7324.

(14) Schmitt, M. A.; Weisblum, B.; Gellman, S. H. Interplay among Folding, Sequence, and Lipophilicity in the Antibacterial and Hemolytic Activities of α-β-Peptides. *J. Am. Chem. Soc.* **2007**, *129*, 417.

(15) Karlsson, A. J.; Pomerantz, W. L.; Gellman, S. H.; Palecek, S. P. Antifungal Activity from 14-Helical β-Peptides. *J. Am. Chem. Soc.* **2006**, *128*, 12630.

(16) Karlsson, A. J.; Pomerantz, W. L.; Neilsen,; J., K.; Gellman, S. H.; Palecek, S. P. Effect of Sequence and Structural Properties on 14-Helical β-Peptide Activity against Candida albicans Planktonic Cells and Biofilms. *ACS Chem. Biol.* **2009**, *4*, 567.

(17) Mahlapuu, M.; Hakansson, J.; Ringstad, L.; Bjrn, C. Antimicrobial Peptides: An Emerging Category of Therapeutic Agents. *Frontiers in Cellular and Infection Microbiology* **2016**, *6*, 194.

(18) Shai, Y. Mode of action of membrane active antimicrobial peptides. *Biopolymers* **2002**, *66*, 236.

(19) Matsuzaki, K. Why and how are peptide?lipid interactions utilized for self-defense? Magainins and tachyplesins as archetypes. *Biochim.Biophys.Acta* **1999**, *1462*, 1.

(20) Leontiadou, H.; Mark, A. E.; Marrink, S. J. antimicrobial peptides in action. *J. Am. Chem. Soc.* **2006**, *128*, 12156.

(21) Sengupta, D.; Leontiadou, H.; Mark, A. E.; Marrink, S. J. Toroidal pores formed by antimicrobial peptides show significant disorder. *Biochim.Biophys. Acta* **2008**, *1778*, 2308.

(22) Perrin, B.; Pastor, R. Simulations of Membrane-Disrupting Peptides I: Alamethicin Pore Stability and Spontaneous Insertion. *Biophysical Journal* **2016**, *111*, 1248 – 1257.

(23) Perrin, B.; Fu, R.; Cotten, M.; Pastor, R. Simulations of Membrane-Disrupting Peptides

II: AMP Piscidin 1 Favors Surface Defects over Pores. *Biophysical Journal* **2016**, *111*, 1258 – 1266.

(24) Murzyn, K.; Rog, T.; Pasenkiewicz-Gierula, M. Phosphatidylethanolamine-Phosphatidylglycerol Bilayer as a Model of the Inner Bacterial Membrane. *Biophysical Journal* **2005**, *88*, 1091 – 1103.

(25) Mukherjee, S.; Kar, R. K.; Nanga, R. P. R.; Mroue, K. H.; Ramamoorthy, A.; Bhunia, A. Accelerated molecular dynamics simulation analysis of MSI-594 in a lipid bilayer. *Phys. Chem. Chem. Phys.* **2017**, *19*, 19289–19299.

(26) Zhao, W.; Rog, T.; Gurtovenko, A. A.; Vattulainen, I.; Karttunen, M. Role of phosphatidylglycerols in the stability of bacterial membranes. *Biochimie* **2008**, *90*, 930 – 938.

(27) Marrink, S. J.; de Vries, A. H.; Mark, A. E. Coarse Grained Model for Semiquantitative Lipid Simulations. *The Journal of Physical Chemistry B* **2004**, *108*, 750–760.

(28) Yesylevskyy, S. O.; Schafer, L. V.; Sengupta, D.; Marrink, S. J. Polarizable Water Model for the Coarse-Grained MARTINI Force Field. *PLOS Computational Biology* **2010**, *6*, 1–17.

(29) Marrink, S. J.; Risselada, H. J.; Yefimov, S.; Tieleman, D. P.; de Vries, A. H. The MARTINI Force Field:a Coarse Grained Model for Biomolecular Simulations. *J. Phys. Chem. B* **2007**, *111*, 7812–7824, PMID: 17569554.

(30) Monticelli, L.; Kandasamy, S. K.; Periole, X.; Larson, R. G.; Tieleman, D. P.; Marrink, S.-J. The MARTINI Coarse-Grained Force Field: Extension to Proteins. *J. Chem. Theory Comput.* **2008**, *4*, 819–834, PMID: 26621095.

(31) Marrink, S. J.; Tieleman, D. P. Perspective on the Martini model. *Chem. Soc. Rev.* **2013**, *42*, 6801–6822.

(32) de Jong, D. H.; Singh, G.; Bennett, W. F. D.; Arnarez, C.; Wassenaar, T. A.; Schafer, L. V.; Periole, X.; Tieleman, D. P.; Marrink, S. J. Improved Parameters for the Martini Coarse-Grained Protein Force Field. *J. Chem. Theory Comput.* **2013**, *9*, 687–697, PMID: 26589065.

(33) Epand, R. F.; Raguse, L.; Gellman, S. H.; Epand, R. M. Antimicrobial 14-Helical beta-Peptides: AÄâ Potent Bilayer Disrupting Agents. *Biochemistry* **2004**, *43*, 9527–9535, PMID: 15260496.

(34) Ludtke, S. J.; He, K.; Heller, W. T.; Harroun, T. A.; Yang, L.; Huang, H. W. Membrane Pores Induced by Magainin. *Biochemistry* **1996**, *35*, 13723–13728, PMID: 8901513.

(35) Miyazaki, Y.; Okazaki, S.; Shinoda, W. Free energy analysis of membrane pore formation process in the presence of multiple melittin peptides. *Biochimica et Biophysica Acta (BBA) - Biomembranes* **2019**, *1861*, 1409 – 1419.

(36) Lipkin, R.; Lazaridis, T. Computational studies of peptide-induced membrane pore formation. *Philosophical Transactions of the Royal Society B: Biological Sciences* **2017**, *372*, 20160219.

(37) Ulmschneider, J. P.; Ulmschneider, M. B. Molecular Dynamics Simulations Are Redefining Our View of Peptides Interacting with Biological Membranes. *Accounts of Chemical Research* **2018**, *51*, 1106–1116, PMID: 29667836.

(38) Irudayam, S. J.; Pobandt, T.; Berkowitz, M. L. Free Energy Barrier for Melittin Reorientation from a Membrane-Bound State to a Transmembrane State. *The Journal of Physical Chemistry B* **2013**, *117*, 13457–13463, PMID: 24117276.

(39) Das, M.; Dahal, U.; Mesele, O.; Liang, D.; Cui, Q. Molecular Dynamics Simulation of Interaction between Functionalized Nanoparticles with Lipid Membranes: Analysis of Coarse-Grained Models. *The Journal of Physical Chemistry B* **2019**, *123*, 10547–10561, PMID: 31675790.

(40) Prieto, L.; He, Y.; Lazaridis, T. Protein Arcs May Form Stable Pores in Lipid Membranes. *Biophysical Journal* **2014**, *106*, 154 – 161.

(41) Awasthi, N.; Hub, J. S. Simulations of Pore Formation in Lipid Membranes: Reaction Coordinates, Convergence, Hysteresis, and Finite-Size Effects. *Journal of Chemical Theory and Computation* **2016**, *12*, 3261–3269, PMID: 27254744.

(42) Mondal, J. A brief appraisal of computational modeling of antimicrobial peptidesÄô activity. *Drug Development Research* **2019**, *80*, 28–32.

(43) Rzepiela, A. J.; Sengupta, D.; Goga, N.; Marrink, S. J. Membrane poration by antimicrobial peptides combining atomistic and coarse-grained descriptions. *Faraday Discuss.* **2010**, *144*, 431–443.

(44) Choi, H.; Chakraborty, S.; Liu, R.; Gellman, S. H.; Weisshaar, J. C. Single-Cell, Time-Resolved Antimicrobial Effects of a Highly Cationic, Random Nylon-3 Copolymer on Live Escherichia coli. *ACS Chemical Biology* **2016**, *11*, 113–120, PMID: 26493221.

(45) Liu, R.; Chen, X.; Falk, S. P.; Masters, K. S.; Weisblum, B.; Gellman, S. H. Nylon-3 Polymers Active against Drug-Resistant Candida albicans Biofilms. *Journal of the American Chemical Society* **2015**, *137*, 2183–2186, PMID: 25650957.

(46) Chakraborty, S.; Liu, R.; Hayouka, Z.; Chen, X.; Ehrhardt, J.; Lu, Q.; Burke, E.; Yang, Y.; Weisblum, B.; Wong, G. C. L.; Masters, K. S.; Gellman, S. H. Ternary Nylon-3 Copolymers as Host-Defense Peptide Mimics: Beyond Hydrophobic and Cationic Subunits. *Journal of the American Chemical Society* **2014**, *136*, 14530–14535, PMID: 25269798.

(47) Zhu, X.; Konig, P.; Gellman, S. H.; Yethiraj, A.; Cui, Q. Establishing Effective Simulation Protocols for β and α-β-Peptides. II. Molecular Mechanical (MM) Model for a Cyclic β-Residue. *J. Phys. Chem. B* **2008**, *112*, 5439.

(48) Zhu, X.; Konig, P.; Hoffman, M.; Yethiraj, A.; Cui, Q. Establishing effective simulation protocols for β?and α-β?peptides. III. Molecular mechanical model for acyclic β?amino acids. *J. Comput. Chem.* **2010**, *31*, 2063.

(49) MacKerell, A. D. et al. All-Atom Empirical Potential for Molecular Modeling and Dynamics Studies of Proteins. *The Journal of Physical Chemistry B* **1998**, *102*, 3586–3616, PMID: 24889800.

(50) Best, R. B.; Zhu, X.; Shim, J.; Lopes, P. E. M.; Mittal, J.; Feig, M.; MacKerell, A. D. Optimization of the Additive CHARMM All-Atom Protein Force Field Targeting Improved Sampling of the Backbone, and Side-Chain and Dihedral Angles. *J.Chem.Theo. Comput.* **2012**, *8*, 3257–3273, PMID: 23341755.

(51) de Jong, D. H.; Baoukina, S.; Ingolfsson, H. I.; Marrink, S. J. Martini straight: Boosting performance using a shorter cutoff and GPUs. *Comput. Phys. Comm.* **2016**, *199*, 1 – 7.

(52) Hess, B.; Kutzner, C.; Van Der Spoel, D.; Lindahl, E. GROMACS 4: algorithms for highly efficient, load-balanced, and scalable molecular simulation. *J.Chem.Theo. Comput.* **2008**, *4*, 435–447.

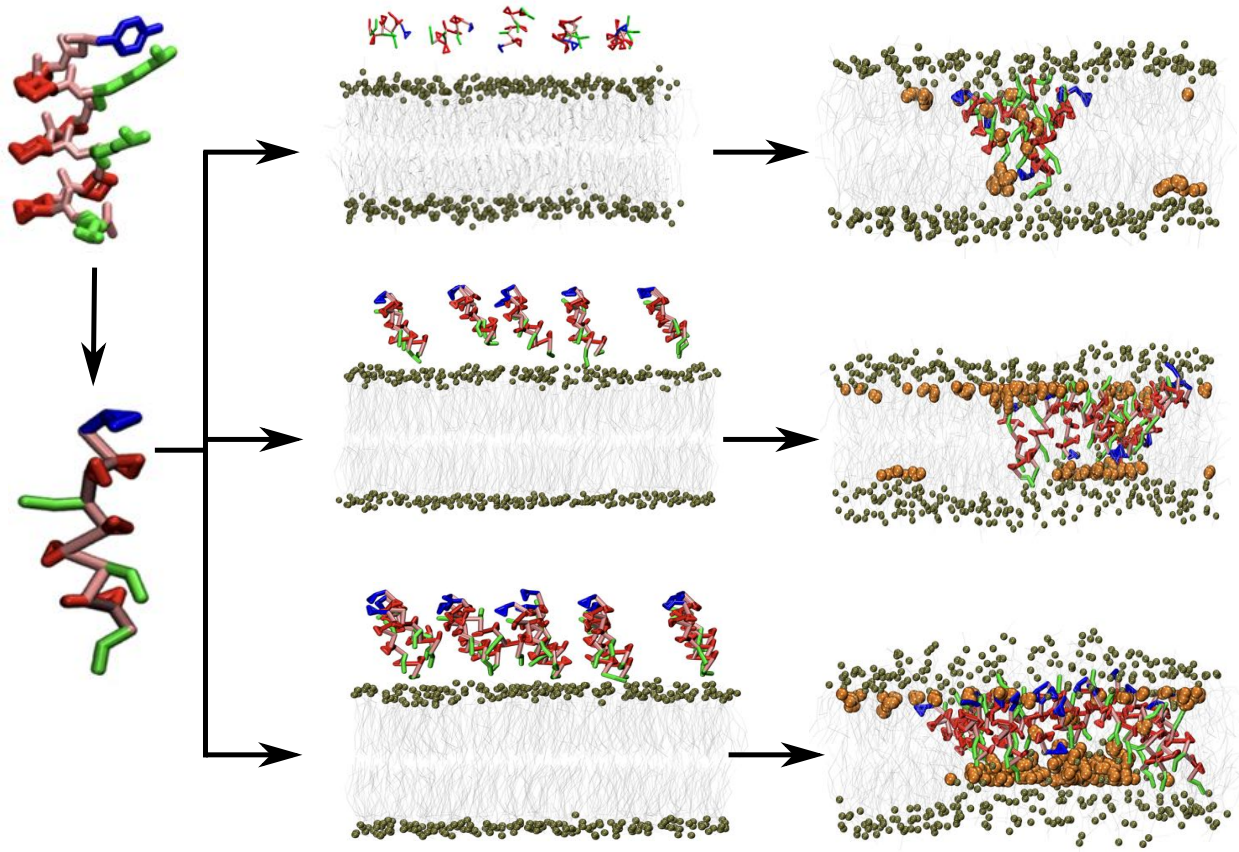

Table of Content